HHS Public Access

Author manuscript

Am J Transplant. Author manuscript; available in PMC 2019 October 01.

Published in final edited form as:

Am J Transplant. 2018 October ; 18(10): 2544–2558. doi:10.1111/ajt.14718.

Myeloid-Derived Suppressor Cells Increase and Inhibit Donor-Reactive T Cell Responses to Graft Intestinal Epithelium in Intestinal Transplant Patients

Shinji Okano[1,2,3], **Kareem Abu-Elmagd**[1], **Danielle D Kish**[2], **Karen Keslar**[2], **William M. Baldwin III**[2], **Robert L. Fairchild**[2], **Masato Fujiki**[1], **Ajai Khanna**[1], **Mohammed Osman**[1], **Guilherme Costa**[1], **John Fung**[1], **Charles Miller**[1], **Hiroto Kayashima**[1], and **Koji Hashimoto**[1]

[1]Transplant Center, Dept. General Surgery, Digestive Disease & Surgery Institute, Cleveland Clinic, Cleveland, Ohio 44195, USA

[2]Dept. Immunology, Lerner Research Institute, Cleveland Clinic, Cleveland, Ohio 44195, USA

Abstract

Recent advances in immunosuppressive regimens have decreased acute cellular rejection (ACR) rates and improved intestinal transplant (ITx) recipient survival. We investigated the role of myeloid-derived suppressor cells (MDSCs) in ITx. We identified MDSCs as $CD33^{+}CD11b^{+}$lineage(CD3/CD56/CD19)$^{-}$HLA-$DR^{-/low}$ cells with 3 subsets, $CD14^{-}CD15^{-}$ (e-MDSC), $CD14^{+}CD15^{-}$ (M-MDSC), and $CD14^{-}CD15^{+}$ (PMN-MDSC), in peripheral blood mononuclear cells (PBMCs) and mononuclear cells in the grafted intestinal mucosa. Total MDSC numbers increased in PBMCs following ITx; among MDSC subsets, M-MDSC numbers were maintained at high level after 2 months following ITx. The MDSC numbers decreased in ITx recipients suffering from ACR. MDSC numbers were positively correlated with serum IL-6 levels and the glucocorticoid administration index. IL-6 and methylprednisolone enhanced the differentiation of bone marrow cells (BMCs) to MDSCs *in vitro*. M-MDSCs and e-MDSCs expressed CCR1, -2, and -3, e-MDSCs and PMN-MDSCs expressed CXCR2, and intestinal grafts expressed the corresponding chemokine ligands following ITx. Of note, the percentage of MDSCs among intestinal mucosal $CD45^{+}$ cells increased after ITx. A novel *in vitro* assay demonstrated that MDSCs suppressed donor-reactive T-cell-mediated destruction of donor intestinal epithelial organoids. Taken together, our results suggest that MDSCs accumulate in the recipient PBMCs and the grafted intestinal mucosa in ITx, and may regulate ACR.

[3]**Address for correspondence:** Shinji Okano M.D., Ph.D., Department of Immunology, Lerner Research Institutes, Cleveland Clinic, 2070 East 90th Street, NB3-30, Cleveland, Ohio 44195, USA. Fax number: +1 216 444 3146, Telephone number: +1 216 444 1230, okanos@ccf.org or okap@surg2.med.kyushu-u.ac.jp.
DR SHINJI OKANO (Orcid ID : 0000-0001-8465-2898)
DR AJAI KHANNA (Orcid ID : 0000-0003-3330-0440)

Disclosure

The authors of this manuscript have no conflicts of interest to disclose, as described by the *American Journal of Transplantation*.

1 Introduction

Intestinal and multivisceral transplantation (ITx) has evolved as the standard treatment for short bowel syndrome and gastrointestinal failure due to congenital and acquired diseases.[1, 2] The intestinal allograft presents a formidable challenge for controlling the alloimmune response. Although the requirement for acute and chronic high-dose immunosuppression had resulted in high patient morbidity and mortality of the patients in the initial era of ITx, the introduction of induction therapy with lymphocyte-depleting agents, such as anti-thymocyte globulin (ATG) and alemtuzumab, has markedly improved short-term graft survival and decreased the incidence and severity of acute cellular rejection (ACR).[3, 4] It has remained unclear whether the positive effects of induction therapy are simply due to decreases in T cell and/or B cell numbers or to the appearance of regulatory components that attenuate recipient responses to the graft.[5] Elucidation of these mechanisms may contribute to the development of new strategies to induce donor-specific immunological tolerance or hyporesponsiveness and improve long-term graft outcomes in ITx.

Myeloid-derived suppressor cells (MDSCs) are a heterogeneous population of cells originally characterized in rodent cancer models and cancer patients that inhibit the immune response to tumors.[6, 7]. MDSCs suppress both the proliferation and effector functions of T cells, B cells, and NK cells and induce regulatory T cells by various mechanisms.[5] During chronic inflammatory conditions, MDSCs develop from immature myeloid cells and accumulate in peripheral tissues and secondary lymphoid organs.[7] Factors inducing MDSC development include cyclooxygenase 2, prostaglandins, stem-cell factor, M-CSF, IL-6, granulocyte/macrophage CSF (GM-CSF), and vascular endothelial growth factor.[7] MDSCs play a critical role in tolerance induction in rodent transplant models, and increases in MDSCs have been reported in human renal transplant patients.[8–11] However, the mechanisms promoting the development of MDSCs and their impact on alloimmune responses in clinical transplantation remain unclear. It is also unclear as to how chronic immunosuppressants administered to human transplant patients affect the differentiation of MDSCs.

We here investigated the identity and accumulation, and the role of MDSCs in ITx.

2 Materials and Methods

2.1 Patients and patient characteristics

Thirty-seven patients who underwent ITx at the Cleveland Clinic Transplant Center from 2009 to 2016 (n = 36) or at the Intestinal Rehabilitation and Transplant Center, University of Pittsburg Medical Center (UPMC) in 2008 and visited the Intensive Care Unit at Cleveland Clinic (n = 1) were enrolled in this study. The clinical study was approved by the regional ethic committee (IRB No. 11-966 and No. 17-471). All participating patients provided informed consent. Additional information is available in Supplementary Materials.

3 Results

3.1 MDSCs increase in peripheral blood mononuclear cells (PBMCs) of patients after ITx

We first investigated whether myeloid cells expressing the MDSC phenotype were present and increased in PBMCs of patients following ITx without histopathological evidence of ACR. The flow cytometry gating strategy excluded doublets and dead cells and MDSCs were identified as lineage^{-}HLADR$^{-/low}$CD33^{+}CD11b^{+} expressing cells (Figure 1*A*), consistent with other reports.[7, 10, 12–14] Within the MDSC population, 3 subsets were identified based on CD14 and CD15 expression: CD14^{+}CD15^{-} monocytic (M-MDSC), CD14^{-}CD15^{+} polymorphonuclear MDSC (PMN-MDSC), and CD14^{-}CD15^{-} early-stage MDSC (e-MDSC) (Figure 1*A*).[13] As reported in previous studies[12, 13, 15–17], M-MDSCs had kidney-shaped nuclei and PMN-MDSC had lobulated nuclei; these MDSCs were relatively smaller than conventional monocytes and granulocytes, respectively (Figure 1*B*). In contrast, e-MDSCs contained a mixture of cells with small round, lobulated, and kidney-shaped nuclei, and the cell size was smaller than that of the other MDSC subsets (Figure 1*B*).

Although small numbers of cells expressing the MDSC phenotype were detected in PBMCs prior to transplant, the total MDSC numbers in PBMCs were significantly increased by 2 months after ITx and maintained past 1 year post-transplant (Figure 1*C and D*). Although levels of each of the MDSC subset were increased following ITx, they showed different patterns. Peripheral blood PMN-MDSC and e-MDSC numbers were significantly increased from pre-transplant levels within 2 months after ITx (Figure 1*E and F*), and e-MDSC numbers were maintained throughout the study period (Figure 1*F*). However, M-MDSC numbers were not significantly increased until 2 months after ITx and then increased after 2 months following ITx (Figure 1*G*). As part of the induction therapy at the time of transplant, 32 of the 37 patients (84%) were treated with alemtuzumab (Campath-1H)-a humanized anti-CD52 mAb, known to be a depleting antibody-which has rapid and long-lasting effects.[18] Therefore, to investigate whether alemtuzumab affect the numbers of MDSC subsets, we assessed CD52 expression on MDSCs. We consistently observed high CD52 expression on M-MDSCs, low-absent expression on PMN-MDSCs, and heterogenous expression on e-MDSCs across the patient samples (Figure S1). Consistent with the CD52 expression, M-MDSCs were detected 4 weeks after transplant in peripheral blood of ITx patients not treated with alemtsuzumab; however, M-MDSCs were not detected in those patients treated with alemtuzumab (Figure S2*A and B*). In serial samples from ITx patients treated with alemtsuzumab, M-MDSCs were detected more than 4 months after ITx when other CD52^{+}lineage(CD3, CD19, and CD56)$^{+}$ cells were detected, but not within a month after ITx (Figure S2*C*). Overall, these findings suggest that the three MDSC subsets increase in the peripheral blood of ITx patients after transplant and that alemtuzumab induction therapy affects the number of M-MDSCs.

Next, the MDSC-phenotype cells isolated from the peripheral blood of ITx patients were tested for the ability to suppress T cell activation. CD33-depleted cells from pre-transplant PBMC samples were used as a source of responder T cells and cultured in anti-CD3/CD28 mAb coated wells, with autologous MDSCs enriched from post-transplant PBMC samples of the same recipient. The MDSCs inhibited both CD4 and CD8 T cell proliferation in

response to anti-CD3/CD28 stimulation (Figure 2A) and IFN-γ production (Table S2). To examine the suppressive activity of each MDSC subset, each subset was sorted on a flow cytometer. Each MDSC subset suppressed T cell proliferation in a dose-dependent manner (Figure 2B).

3.2 Exogenous steroid hormone enhances expansion of MDSCs from human bone marrow cells (BMCs)

Since GM-CSF and pro-inflammatory cytokines, such as tumor necrosis factor-α (TNF-α) and interleukin-6 (IL-6), induce MDSC expansion in tumor rodent models[7], we investigated whether these factors contribute to MDSC accumulation in ITx patients and determined the plasma levels of IL-6, TNF-α, and GM-CSF and their relationship to peripheral blood MDSC numbers. Plasma IL-6 levels, but not those of TNF-α and GM-CSF, were correlated significantly with MDSC numbers in PBMCs (Figure 3A; $r = 0.6888$, $p = 0.0278$ vs. 0.3638 and 0.1942, respectively). In addition, we investigated the correlations of MDSC numbers in PBMCs with the days after ITx, tacrolimus trough levels and administered doses of exogenous steroids per body weight, which was normalized to a value based on the potency of each steroid drug (Table S3). MDSC numbers were positively correlated with the exogenous steroid dose ($P = 0.0013$) and negatively with tacrolimus trough levels ($P < 0.0001$). In contrast to the significant increases in MDSC numbers in peripheral blood prior to vs. following transplantation (Figure 1*D*), no significant correlation was observed between MDSC numbers and the days after ITx (Figure 3B).

These results led us to hypothesize that serum IL-6 and exogenous steroid induce MDSC expansion. Whereas PBMC from healthy volunteers cultured with IL-6 and methylprednisolone (MP) did not result in MDSC expansion (Figure S3), IL-6 and MP enhanced the numbers of MDSC-phenotype cells when BMCs from healthy volunteers were cultured in basic medium supplemented with G-CSF and GM-CSF (Figure 3*C*, Figure S4). MP was more potent than IL-6 in expanding the MDSCs (Figure 3*C*), and the effect of MP was dose dependent (Figure 3*D*). Mifepristone-a glucocorticoid receptor antagonist-abrogated the effect of MP (Figure 3*E*). MDSCs generated from BMCs grown with IL-6 and MP suppressed both autologous CD4 and CD8 T cell proliferation in cultures with allogeneic B cells (Figure 3*F and G*) and IFN-γ production (Figure 3*H*).

3.3 Positive correlation between MDSCs and regulatory T cell (Treg) in ITx recipients

In kidney transplant recipients, MDSCs induce $FoxP3^+CD4^+$ T cell proliferation.[19] Therefore, we investigated the relation between peripheral blood MDSCs and total regulatory $CD3^+CD4^+CD25^+CD127^-Foxp3^+$ Treg numbers (Figure 4*A*). In this study, we also dissected subsets of Treg based on Helios expression, which was preferably expressed in naturally occurring regulatory CD4 T cells,[20–23] and examined the relations between MDSCs and the numbers of cells in subsets of Treg (Figure 4*A*). The numbers of total, $Helios^+$ and $Helios^-$ Treg cells in PBMCs of ITx patients were correlated with MDSC numbers (Figure 4*B*: $r = 0.5584$, $p = 0.0056$; 4*C*: $r = 0.4622$, $p = 0.0263$; and 4*D*: $r = 0.6029$, $p = 0.$ 0.0023, respectively).

3.4 MDSCs increase in the allograft intestinal mucosa

To investigate whether MDSCs infiltrate into transplanted grafts, mononuclear cells from lamina propria components (LPC) were analyzed using flow cytometry. MDSC levels were low or undetectable in the allograft mucosa before implantation, but they significantly increased in percentage among $CD45^+$ cells following ITx (Supplementary Figure 5, Figure 5*A*). For each MDSC subset, the percentages of each of the three MDSC subsets increased in the graft biopsies in the first 12-month period following ITx; however, similar to the PBMCs of the recipients, a minimal increase in M-MDSCs within the first 2 months after ITx was evident compared with the graft infiltration of the other two subsets (Figure 5*B–D*).

To investigate potential mechanisms directing MDSCs into transplanted intestinal grafts, comprehensive chemokine RNA levels were assessed on the NanoStrings® platform. Since distinct MDSC populations were detectable in the intestinal mucosa of grafts after ITx, we focused on chemokines upregulated following ITx. We detected two clusters of chemokine RNA expression levels, including CCL25, CCL15, CXCL6, CCL28, CXCL16, and CCL11, upregulated following ITx (Figure S6). Therefore, MDSC subsets in PBMCs were labeled with antibodies to the corresponding chemokine receptors, including CCR1, CCR2, CCR3, CCR7, CCR9, CXCR2, CXCR6, and β7 integrin, and analyzed by flow cytometry (Figure 5*E*). M-MDSCs showed strong expression of CCR1 and CCR2 and weak expression of CCR3, e-MDSCs showed weak expression of CCR1 but strong expression of CCR2 and CCR3, and PMN-MDSCs did not express these chemokine receptors. In contrast, PMN-MDSCs and some e-MDSCs showed strong expression of CXCR2, whereas M-MDSCs did not. None of the MDSC subsets expressed CXCR6, CCR7, CCR9, or β7 integrin. Graft expression of the CCR1 and CCR3 ligand CCL15 increased approximately 3-fold at 3 months post-transplant, and this expression level was maintained through 6 months post-transplant (Figure 5*F*). Expression of the CCR3 ligand CCL11 was low at the time of transplant and at 3 months post-transplant; however, it was markedly increased at 6 months post-transplant (Figure 5*F*). In contrast, expression levels of other CCR1, CCR2 and CCR3 ligands were as follows: CCL7, CCL16, CCL26 levels were low in allografts before and after transplant, CCL2, CCL3 and CCL23 levels were low in allografts following transplant, and there was no significant increase in the expression levels of CCL5, CCL8, CCL13, CCL14, CCL24, and CCL28 following transplant (Figure 5*F* and figure S6). Graft expression of CXCR2 ligands CXCL1, CXCL2, CXCL3 and IL-8 decreased to near absent levels following transplant when tested at 3 and 6 months post-transplant. However, graft expression of the CXCR2 ligand CXCL6 was low at the time of transplant and increased more than 3-fold by 3 months post-transplant (Figure 5*F* and figure S6). Expression of the IFN-γ inducible chemokines CXCL9, CXCL10 and CXCL11 that direct recruitment of alloantigen-primed T cells did not increase following the transplant (Figure S6). Overall, these results support a role for CCL11 and CCL15 in directing the recruitment of CCR1- and CCR3-expressing M-MDSCs and e-MDSCs and a role for CXCL6 in directing the recruitment of CXCR2-expressing PMN-MDSCs and e-MDSCs into the intestinal grafts following transplant.

3.5 Reduced peripheral blood MDSCs during ACR

The relationship between peripheral blood MDSC numbers and occurrence of ACR was investigated in samples from 9 ITx patients with biopsy-proven ACR. The total numbers of MDSCs in PBMCs from ITx recipients suffering from ACR was significantly lower than those in patients without ACR (Figure 6*A*). ACR occurring within the first two months following transplant had no significant effect on the numbers of MDSC in the peripheral blood; however, the numbers of PMN-MDSCs during ACR tended to be lower than those in patients without ACR (Figure 6*B*). However, the numbers of M-MDSCs and e-MDSCs, but not PMN-MDSCs, significantly decreased in PBMCs from ITx patients experiencing ACR 2 months or more after transplant compared to those in patients without ACR (Figure 6*B*). In terms of clinical characteristics and demographics of the ITx patients, while de novo DSA was detected at higher rates in patients suffering from ACR than in patients without ACR, there was no significant correlation between patients with ACR and without ACR in the other factors (Table S4).

3.6 MDSCs suppress donor-specific T cell-mediated damage of intestinal epithelial organoids

A critical histological criterion for diagnosis of ACR is more than 6 apoptotic bodies/10 sequential crypts,[24, 25] which is proposed to reflect donor-reactive T cell-mediated epithelial damage.[26] To directly investigate the role of MDSCs in ACR, we established an *ex vivo* co-culture system, called “organoid formation assay”, using donor-reactive T cells and intestinal epithelial organoids from donor intestinal grafts. Donor-reactive T cells ($CFSE^{low}$ T cells) and non-donor-reactive T cells ($CFSE^{high}$ T cells) were sorted after 6 days of co-culture with irradiated donor B cells (Figure 7*A*). Subsequently, epithelial organoids derived from donor intestinal grafts, were co-cultured with $CFSE^{low}$ T cells or $CFSE^{high}$ T cells in the presence or absence of the sorted recipient MDSCs for 5 days. The number of viable epithelial organoids was significantly less in the presence of donor-reactive T cells compared to that in the presence of non-donor-reactive T cells (Figure 7*B and C*), suggesting that the epithelial damage was mediated by donor-specific T cell response. It is noteworthy that the number of viable organoids in the co-cultures with MDSCs and donor-reactive T cells was comparable to that of organoids without T cells, suggesting that MDSCs suppress the damage to organoids by donor-reactive T cells (Figure 7*B and C*). These findings suggest that accumulated MDSCs suppress donor-reactive T cell response to the donor intestinal epithelium.

4 Discussion

In this study, we first demonstrated the key features of MDSCs in clinical ITx: i) Three distinct populations of MDSCs began to increase in the recipient peripheral blood early after ITx, and each subpopulation had the ability to suppress T cell activation. ii) Although PMN-MDSC numbers were increased within 2 months following ITx, M-MDSC and e-MDSC numbers were increased and maintained at high levels in PBMCs after 2 months following ITx; the differences in the number of each MDSC subset during the early period after ITx could be affected by administration of alemtuzumab, as M-MDSCs, but not PMN-MDSCs, expressed CD52 and M-MDSCs were rarely detected in PBMCs of patients, who received

alemtuzumab, during the early period after ITx. iii) The number of MDSCs was significantly correlated with plasma IL-6 levels and administered exogenous glucocorticoid doses, and MP markedly enhanced propagation of MDSCs in BMC cultures. iv) The numbers of Treg cells, including both inducible and naturally occurring Treg cells, was significantly correlated with MDSC numbers. v) The frequency of MDSCs among $CD45^+$ cells was increased in the intestinal allograft mucosa; the percentages of PMN-MDSC and e-MDSC were increased during the first 2 months after ITx, and those of M-MDSC and e-MDSC were increased thereafter, and these graft infiltrating MDSCs expressed chemokine receptors responsive to chemokines expressed by the allograft mucosa. vi) ACR episodes were accompanied by decreases in MDSC levels. vii) Using a novel *ex vivo* ACR assay, MDSCs suppressed the ability of donor-specific T cells to mediate donor intestinal epithelial organoid damage. Overall, these results suggest that exogenous glucocorticoid promote MDSC differentiation from BMCs and their accumulation in the recipient peripheral blood and donor graft intestinal mucosa to regulate the characteristic T cell-mediated destruction of the graft epithelium. Among MDSC subpopulations, M-MDSCs may play more important roles in control of ACR of intestinal grafts, especially in late period after ITx, than the others.

Numerous factors that contribute to the differentiation and expansion of MDSCs, have been reported.[7,27–30] The MDSCs may have an almost entirely recipient-derived origin, as macrochimerism of myeloid cells is hard to detect in intestinal transplantation,[31, 32] which we also confirmed in some of the recipients (data not shown). In this study, we demonstrated that MP expand MDSCs from human bone marrow cells, but not from PBMCs. Notably, previous rodent models have demonstrated that glucocorticoids enhance the accumulation of MDSCs;[33, 34] however, this study is the first to demonstrate that glucocorticoids enhance the expansion of human MDSCs in a dose-dependent manner by GR signaling in BMC cultures. Maximal numbers of MDSCs in the BMC culture were observed with treatment of 1 μM of MP (Figure 3D), which corresponds to the peak level in a 70-kg patient given an intravenous dose of 50 mg of MP (0.756 mg/kg) or to the 24-hour trough level following a 30-mg/kg intravenous dose.[35, 36] The latter dose is similar to that used in MP-pulse treatment in ITx. Moreover, on day 3 after MP-pulse treatment for ACR in an ITx patient, the number of MDSCs in PBMCs increased to 6 times the levels observed before treatment (data not shown). Therefore, the use of glucocorticoid drugs to maintain immunosuppression and treat ACR may drive MDSC accumulation in patients following ITx, in addition to the known effects, such as downregulation of effector molecules and induction of effector cell apoptosis, especially in T cells.[36] In terms of calcineurin inhibitors, although the trough levels were negatively correlated with MDSC numbers, addition of FK506 to the BMC culture did not affect the numbers of MDSCs (Figure S7). Since Wang et al. reported that a calcineurin inhibitor, cyclosporine, enhanced infiltration of MDSCs in skin grafts and apoptosis[37], inhibition of the calcineurin-nuclear factor of activated T cells (NFAT) axis may promote MDSC migration toward intestinal grafts rather than MDSC differentiation from bone marrow stem cells, resulting in decreased numbers of MDSCs in PBMCs.

MDSCs migrate not only to secondary lymphoid organs but also to effector sites, such as transplanted grafts and tumors, creating an immunosuppressive environment in rodent models.[9, 38–40, 7, 14] This MDSC migratory potential is essential for tolerance induction in a

heart transplantation model.[9] While there is growing evidence for chemokine signaling in MDSC recruitment to tumor sites,[40] the mechanisms of MDSC migration in infection, autoimmune disease, and transplantation remain unclear. Recently, Pallett et al. reported that PMN-MDSCs potentially utilize signaling through CCR2, CXCR1, and CXCR3 to infiltrate liver tissue following HBV infection to regulate metabolism in the liver, although they did not determine the expression of the respective chemokine ligands in the liver tissue during this recruitment.[41] We demonstrated that all MDSC subsets were detected in intestinal grafts following transplantation and that the percentages of MDSCs among $CD45^+$ cells significantly increased compared to those in pre-transplant grafts. This study is the first to demonstrate accumulation of MDSC in the transplanted organ of human patients. In intestinal graft protocol biopsies, etiology-unknown neutrophilic infiltration in the intestinal mucosa of transplanted grafts is often observed, and the infiltrating neutrophil-like cells are smaller than conventional neutrophils. Our results imply that infiltrating PMN-MDSCs may be detected as neutrophilic infiltration in some cases. Of note, unique chemokine ligand profiles were observed in intestinal grafts following ITx (Figure 5F) and that MDSCs expressed inflammatory chemokine receptors binding these mediators, including CCR1, CCR2, CCR3 and CXCR2 (Figure 5E).

Thus far, it has been unclear whether MDSCs regulate immune responses within effector sites. The lack of clinically relevant model systems for investigation *in vivo* immune responses is a major obstacle toward understanding MDSC function in peripheral non-lymphoid organs in transplantation. Our findings that MDSC levels increase in PBMCs and intestinal grafts in patients without rejection coupled with the low number of MDSCs observed during ACR led us to hypothesize that MDSCs may directly suppress donor-reactive T cell responses to intestinal grafts. Recent development of new 3D organoid culture methods[42–46] allow us to evaluate MDSC function in the transplanted intestinal mucosa. Consistent with our initial hypothesis, our *ex vivo* rejection model revealed that MDSCs suppressed donor-reactive T cell-mediated damages of donor-derived intestinal epithelial organoids. Our findings suggest that balance between donor-reactive T cell responses and their suppression by MDSCs may impact the occurrence of ACR; during ACR, MDSC activities may be overwhelmed by donor-reactive T cell responses, or decreased number of MDSCs may allow donor-reactive T cells to induce ACR. This hypothesis warrants further study to determine the molecular mechanisms underlying MDSC-mediated immunomodulation within ITx grafts. Furthermore, it will be of interest to investigate the role of other components, such as stromal cells, secreted molecules or extracellular matrix, that may affect MDSC function.

Our study has certain methodological limitations. Although monocytes and M-MDSCs can be distinguished on the basis of expression of MHC class II molecules, there remains difficulty in separating PMN-MDSCs from neutrophils based on surface markers. Therefore, density separation or functional studies are needed to distinguish between PMN-MDSCs and neutrophils.[12, 17] Although we obtained PBMCs using Ficoll-separation medium, small numbers of mononuclear cells from biopsy samples prevented us from performing the density separation. It was also difficult to obtain sufficient quantities of peripheral PBMCs and graft infiltrating cells of intestinal transplant patients to investigate MDSC functions in multiple replicate of samples or in all the patients, as the patients were usually subjected to

heavy immunosuppressive conditions, especially during the early time period following transplantation. Next, the sample size is relatively small, and we need to confirm our findings using a multi-center study. Finally, it was also difficult to investigate the spatiotemporal distribution of MDSCs in the body of each patient. Rodent intestinal transplantation models may be useful to identify critical chemokines and chemokine receptors in future experiments.

Finally, follow-up histological studies of graft biopsies from ITx patients without clinically evident ACR demonstrated variable levels of apoptosis, epithelial cell regeneration, and mononuclear cell infiltration. Therefore, it is expected that subclinical ACR responses may intermittently or continuously emerge even after induction therapy for ITx. MDSCs may be crucial in controlling the subclinical ACR and preventing the occurrence of clinically evident ACR within the graft mucosa through mechanisms facilitating MDSC differentiation from BMCs and MDSC recruitment to intestinal grafts via distinct chemokine ligand-chemokine receptor interactions in ITx. Garcia, et al. suggest that MDSCs play a critical role in suppressing the T cell response to donor antigens in the graft sites prior to the establishment of immunological tolerance to donor grafts.[9] In ITx, donor-specific T cell hyporesponsiveness is frequently observed in intestinal transplant patients without rejection following a long lapse of ITx with induction therapy (data not shown).[47] Overall, our findings support the hypothesis that MDSCs play an important role in bridging to donor-specific T cell hyporesponsive states in clinical ITx, as observed in rodent models,[9] and provide strong evidence that MDSCs can function to directly suppress pathogenic T cell responses to the epithelium in the context of ITx.

Supplementary Material

Refer to Web version on PubMed Central for supplementary material.

Acknowledgments

We thank Drs. Mansour A Parsi, MD, Gregory Zuccaro Jr., MD, Menon, K V Narayanan, MD, Ibrahim Hanouneh, Robert S O Shea, Amit Bhatt, MD, Abdullah S Shatnawei, MD, Bradley D Confer, MD, Carlos Romero-Marrero, MD, Prashanthi Thota, MD, and all the staff in the Department of Gastroenterology and Hepatology, for sampling of intestinal biopsies.

We thank Ana Bennett, MD, Lisa Yerian, MD, Deepa Patil, MD, and all the GI pathology staff at the Department of Pathology.

We thank Bookie Min and DR. J for assistance with flow cytometry.

We thank Nina Dvorina M.D., B. S. for technical assistance with Giemsa staining.

We thank Kewal Asosingh PhD, Joseph Gerow, BS, and Eric Schultz, BS for assistance with analysis of flow cytometry and flow sorting in the flow cytometry core.

We thank Raw Lisa, MSN, Natasha Raush, BSN, Christine Wagner, RNC, Shatina Roddy, RN, Cindy Shovary, RN, BSN, Anita Barowski, RN, MS, Neha Parekh, MS, RD, LD, CNSC, Suzanne Himes, RN, BSN, Elizabeth Lennon, MS, PA-C, RD for assistance as transplant coordinators and mid-level practitioners.

We thank Daniel Zwick and Sreedevi Goparaju for English proof reading and editing figures, respectively.

This work was supported by a grant from the Research Program Committee, Cleveland Clinic RPC 2011-1015 (K.H) and NIH RO1-AI40459 (R.L.F).

Nonstandard abbreviations used in this paper

ITx	Intestinal and multivisceral transplantation
Itx	Isolated intestinal transplantation
MV	Multivisceral transplantation
ATG	Anti-thymocyte globulin
ACR	Acute cellular rejection
MDSC(s)	Myeloid-derived suppressor cell(s)
GM-CSF	Granulocyte/macrophage CSF
PBMCs	Peripheral blood mononuclear cells
M-MDSC	$CD14^{+}CD15^{-}$ MDSC
PMN-MDSC	$CD14^{-}CD15^{+}$ MDSC
e-MDSC	$CD14^{-}CD15^{-}$ MDSC
BMCs	Bone marrow cells
TNF-α	Tumor necrosis factor-α
IL-6	Interleukin-6
MP	Methylprednisolone
G-CSF	Granulocyte CSF
Treg	Regulatory T cells
LPC	Lamina propria components

References

1. Abu-Elmagd K. The concept of gut rehabilitation and the future of visceral transplantation. Nature reviews Gastroenterology & hepatology. 2015; 12(2):108–120. [PubMed: 25601664]
2. Hashimoto K, Costa G, Khanna A, et al. Recent Advances in Intestinal and Multivisceral Transplantation. Adv Surg. 2015; 49(1):31–63. [PubMed: 26299489]
3. Abu-Elmagd KM, Costa G, Bond GJ, et al. Evolution of the immunosuppressive strategies for the intestinal and multivisceral recipients with special reference to allograft immunity and achievement of partial tolerance. Transpl Int. 2009; 22(1):96–109. [PubMed: 18954362]
4. Lauro A, Zanfi C, Bagni A, et al. Induction therapy in adult intestinal transplantation: reduced incidence of rejection with "2-dose" alemtuzumab protocol. Clinical transplantation. 2013; 27(4): 567–570. [PubMed: 23815302]
5. Wood KJ, Bushell A, Hester J. Regulatory immune cells in transplantation. Nat Rev Immunol. 2012; 12(6):417–430. [PubMed: 22627860]
6. Almand B, Clark JI, Nikitina E, et al. Increased production of immature myeloid cells in cancer patients: a mechanism of immunosuppression in cancer. J Immunol. 2001; 166(1):678–689. [PubMed: 11123353]

7. Gabrilovich DI, Nagaraj S. Myeloid-derived suppressor cells as regulators of the immune system. Nat Rev Immunol. 2009; 9(3):162–174. [PubMed: 19197294]
8. Dugast AS, Haudebourg T, Coulon F, et al. Myeloid-derived suppressor cells accumulate in kidney allograft tolerance and specifically suppress effector T cell expansion. J Immunol. 2008; 180(12): 7898–7906. [PubMed: 18523253]
9. Garcia MR, Ledgerwood L, Yang Y, et al. Monocytic suppressive cells mediate cardiovascular transplantation tolerance in mice. J Clin Invest. 2010; 120(7):2486–2496. [PubMed: 20551515]
10. Luan Y, Mosheir E, Menon MC, et al. Monocytic myeloid-derived suppressor cells accumulate in renal transplant patients and mediate CD4(+) Foxp3(+) Treg expansion. Am J Transplant. 2013; 13(12):3123–3131. [PubMed: 24103111]
11. Thomson AW, Turnquist HR. Regulators with potential: substantiating myeloid-derived suppressor cells in human organ transplantation. Am J Transplant. 2013; 13(12):3061–3062. [PubMed: 24102710]
12. Bronte V, Brandau S, Chen SH, et al. Recommendations for myeloid-derived suppressor cell nomenclature and characterization standards. Nat Commun. 2016; 7:12150. [PubMed: 27381735]
13. Gustafson MP, Lin Y, Maas ML, et al. A method for identification and analysis of non-overlapping myeloid immunophenotypes in humans. PLoS One. 2015; 10(3):e0121546. [PubMed: 25799053]
14. Talmadge JE, Gabrilovich DI. History of myeloid-derived suppressor cells. Nat Rev Cancer. 2013; 13(10):739–752. [PubMed: 24060865]
15. Gorgun GT, Whitehill G, Anderson JL, et al. Tumor-promoting immune-suppressive myeloid-derived suppressor cells in the multiple myeloma microenvironment in humans. Blood. 2013; 121(15):2975–2987. [PubMed: 23321256]
16. Gros A, Turcotte S, Wunderlich JR, et al. Myeloid cells obtained from the blood but not from the tumor can suppress T-cell proliferation in patients with melanoma. Clin Cancer Res. 2012; 18(19): 5212–5223. [PubMed: 22837179]
17. Veglia F, Perego M, Gabrilovich D. Myeloid-derived suppressor cells coming of age. Nat Immunol. 2018; 19(2):108–119. [PubMed: 29348500]
18. Kirk AD, Hale DA, Mannon RB, et al. Results from a human renal allograft tolerance trial evaluating the humanized CD52-specific monoclonal antibody alemtuzumab (CAMPATH-1H). Transplantation. 2003; 76(1):120–129. [PubMed: 12865797]
19. Huang B, Pan PY, Li Q, et al. Gr-1+CD115+ immature myeloid suppressor cells mediate the development of tumor-induced T regulatory cells and T-cell anergy in tumor-bearing host. Cancer Res. 2006; 66(2):1123–1131. [PubMed: 16424049]
20. Liu W, Putnam AL, Xu-Yu Z, et al. CD127 expression inversely correlates with FoxP3 and suppressive function of human CD4+ T reg cells. J Exp Med. 2006; 203(7):1701–1711. [PubMed: 16818678]
21. Hill JA, Feuerer M, Tash K, et al. Foxp3 transcription-factor-dependent and -independent regulation of the regulatory T cell transcriptional signature. Immunity. 2007; 27(5):786–800. [PubMed: 18024188]
22. Thornton AM, Korty PE, Tran DQ, et al. Expression of Helios, an Ikaros transcription factor family member, differentiates thymic-derived from peripherally induced Foxp3+ T regulatory cells. J Immunol. 2010; 184(7):3433–3441. [PubMed: 20181882]
23. Getnet D, Grosso JF, Goldberg MV, et al. A role for the transcription factor Helios in human CD4(+)CD25(+) regulatory T cells. Mol Immunol. 2010; 47(7–8):1595–1600. [PubMed: 20226531]
24. Wu T, Abu-Elmagd K, Bond G, et al. A schema for histologic grading of small intestine allograft acute rejection. Transplantation. 2003; 75(8):1241–1248. [PubMed: 12717210]
25. Garcia M, Delacruz V, Ortiz R, et al. Acute cellular rejection grading scheme for human gastric allografts. Hum Pathol. 2004; 35(3):343–349. [PubMed: 15017591]
26. Fishbein TM. Intestinal transplantation. The New England journal of medicine. 2009; 361(10): 998–1008. [PubMed: 19726774]
27. Waight JD, Netherby C, Hensen ML, et al. Myeloid-derived suppressor cell development is regulated by a STAT/IRF-8 axis. J Clin Invest. 2013; 123(10):4464–4478. [PubMed: 24091328]

28. Marigo I, Bosio E, Solito S, et al. Tumor-induced tolerance and immune suppression depend on the C/EBPbeta transcription factor. Immunity. 2010; 32(6):790–802. [PubMed: 20605485]
29. Kawano M, Mabuchi S, Matsumoto Y, et al. The significance of G-CSF expression and myeloid-derived suppressor cells in the chemoresistance of uterine cervical cancer. Sci Rep. 2015; 5:18217. [PubMed: 26666576]
30. Sumida K, Wakita D, Narita Y, et al. Anti-IL-6 receptor mAb eliminates myeloid-derived suppressor cells and inhibits tumor growth by enhancing T-cell responses. Eur J Immunol. 2012; 42(8):2060–2072. [PubMed: 22653638]
31. Zuber J, Rosen S, Shonts B, et al. Macrochimerism in Intestinal Transplantation: Association With Lower Rejection Rates and Multivisceral Transplants, Without GVHD. Am J Transplant. 2015; 15(10):2691–2703. [PubMed: 25988811]
32. Zuber J, Shonts B, Lau SP, et al. Bidirectional intragraft alloreactivity drives the repopulation of human intestinal allografts and correlates with clinical outcome. Sci Immunol. 2016; 1(4)
33. Liao J, Wang X, Bi Y, et al. Dexamethasone potentiates myeloid-derived suppressor cell function in prolonging allograft survival through nitric oxide. J Leukoc Biol. 2014; 96(5):675–684. [PubMed: 24948701]
34. Varga G, Ehrchen J, Tsianakas A, et al. Glucocorticoids induce an activated, anti-inflammatory monocyte subset in mice that resembles myeloid-derived suppressor cells. J Leukoc Biol. 2008; 84(3):644–650. [PubMed: 18611985]
35. Al-Habet SM, Rogers HJ. Methylprednisolone pharmacokinetics after intravenous and oral administration. Br J Clin Pharmacol. 1989; 27(3):285–290. [PubMed: 2655680]
36. Davis TE, Kis-Toth K, Szanto A, et al. Glucocorticoids suppress T cell function by up-regulating microRNA-98. Arthritis Rheum. 2013; 65(7):1882–1890. [PubMed: 23575983]
37. Wang X, Bi Y, Xue L, et al. The calcineurin-NFAT axis controls allograft immunity in myeloid-derived suppressor cells through reprogramming T cell differentiation. Mol Cell Biol. 2015; 35(3): 598–609. [PubMed: 25452304]
38. Qin J, Arakawa Y, Morita M, et al. C-C Chemokine Receptor type 2 (CCR2)-Dependent Migration of Myeloid-Derived Suppressor Cells in Protection of Islet Transplants. Transplantation. 2016
39. Motz GT, Coukos G. Deciphering and reversing tumor immune suppression. Immunity. 2013; 39(1):61–73. [PubMed: 23890064]
40. Kumar V, Patel S, Tcyganov E, et al. The Nature of Myeloid-Derived Suppressor Cells in the Tumor Microenvironment. Trends Immunol. 2016; 37(3):208–220. [PubMed: 26858199]
41. Pallett LJ, Gill US, Quaglia A, et al. Metabolic regulation of hepatitis B immunopathology by myeloid-derived suppressor cells. Nat Med. 2015; 21(6):591–600. [PubMed: 25962123]
42. Fatehullah A, Tan SH, Barker N. Organoids as an in vitro model of human development and disease. Nat Cell Biol. 2016; 18(3):246–254. [PubMed: 26911908]
43. Sato T, van Es JH, Snippert HJ, et al. Paneth cells constitute the niche for Lgr5 stem cells in intestinal crypts. Nature. 2011; 469(7330):415–418. [PubMed: 21113151]
44. Sato T, Vries RG, Snippert HJ, et al. Single Lgr5 stem cells build crypt-villus structures in vitro without a mesenchymal niche. Nature. 2009; 459(7244):262–265. [PubMed: 19329995]
45. Sato T, Stange DE, Ferrante M, et al. Long-term expansion of epithelial organoids from human colon, adenoma, adenocarcinoma, and Barrett's epithelium. Gastroenterology. 2011; 141(5):1762–1772. [PubMed: 21889923]
46. Lindemans CA, Calafiore M, Mertelsmann AM, et al. Interleukin-22 promotes intestinal-stem-cell-mediated epithelial regeneration. Nature. 2015; 528(7583):560–564. [PubMed: 26649819]
47. Mathew JM, Tryphonopoulos P, DeFaria W, et al. Role of innate and acquired immune mechanisms in clinical intestinal transplant rejection. Transplantation. 2015; 99(6):1273–1281. [PubMed: 25539468]

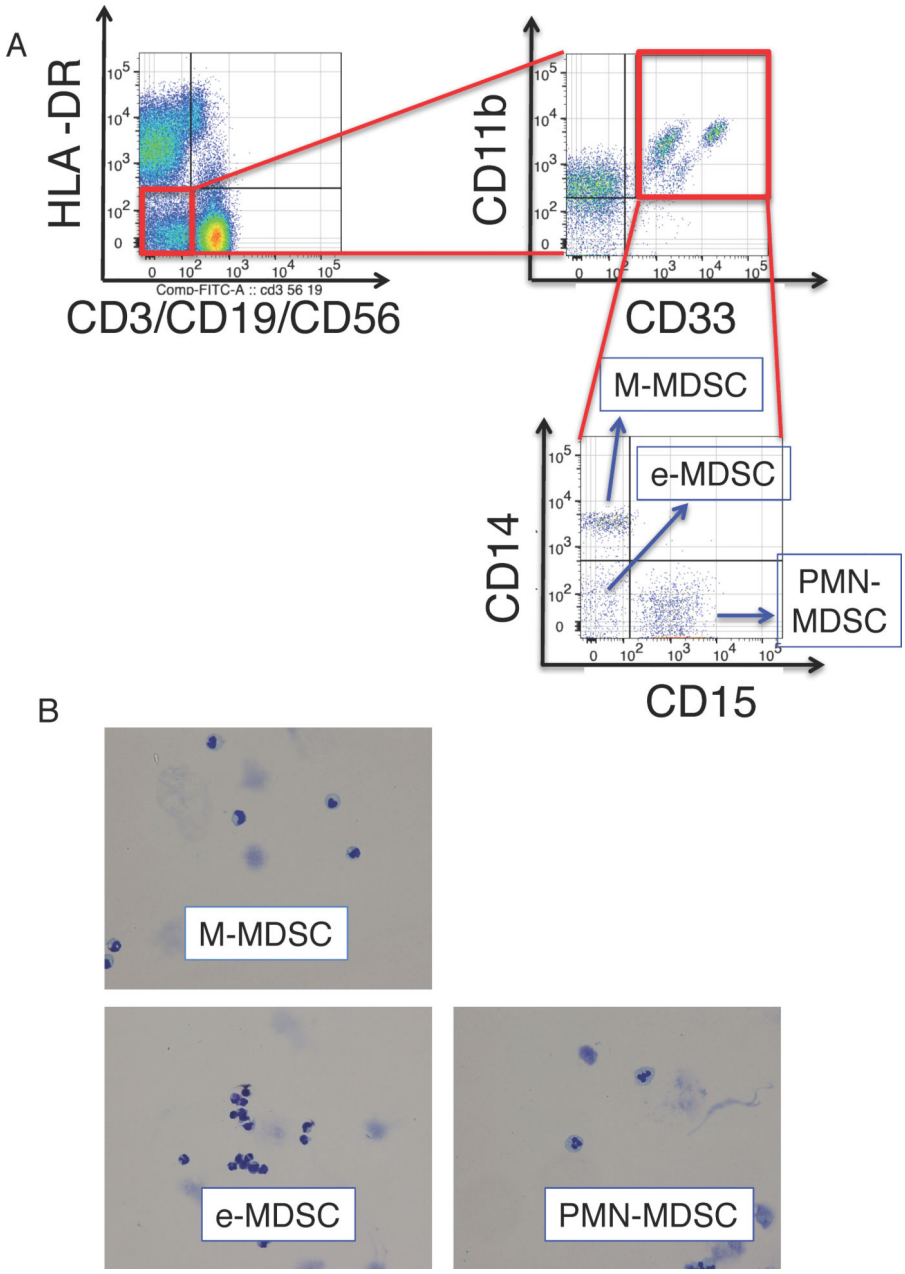

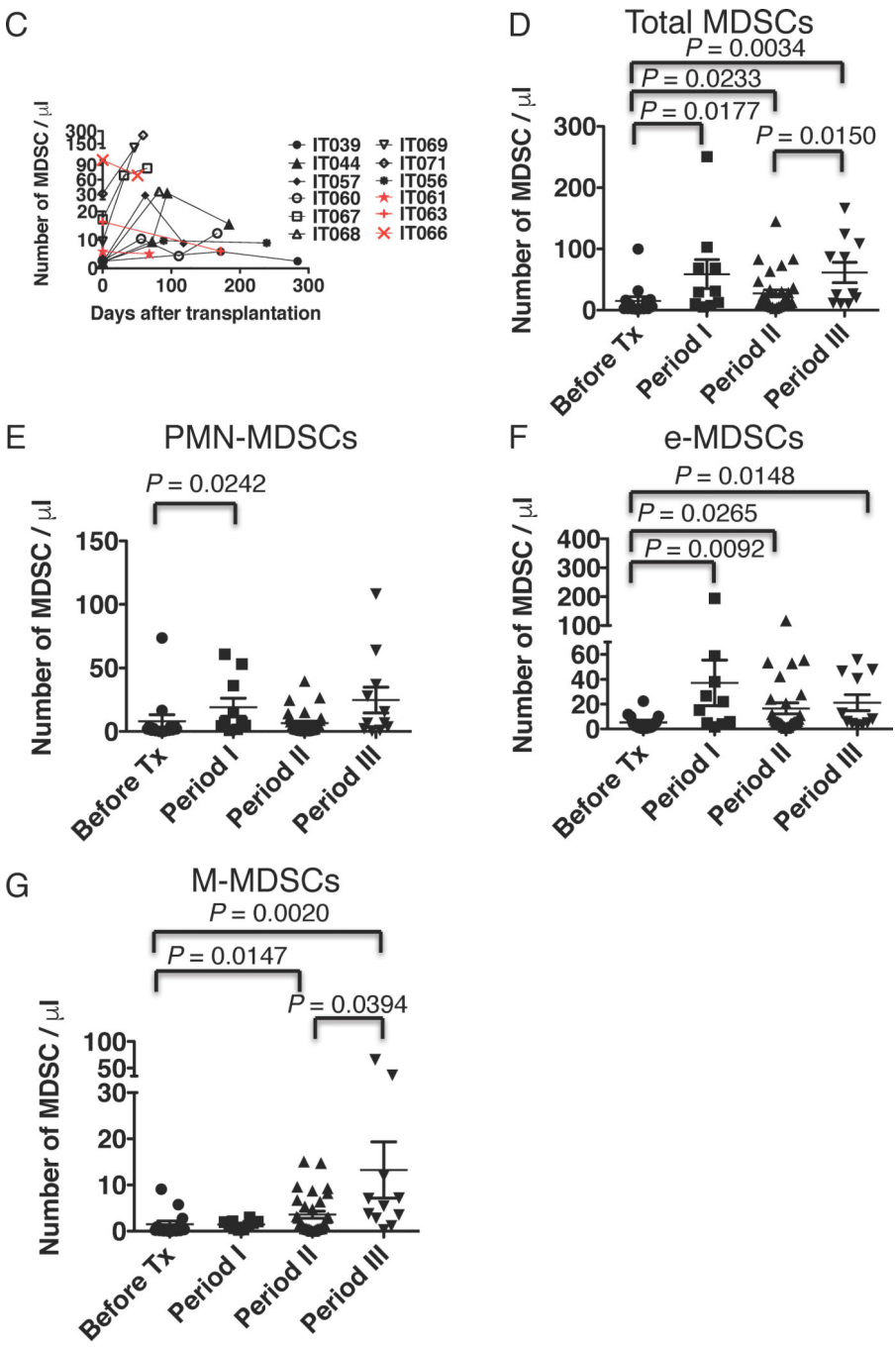

Figure 1. Phenotypes of MDSCs and increase in MDSCs in IT patients

(A) The PBMCs were stained with fluorescent-labelled antibodies and analyzed using flow cytometry. The obtained cells were gated on an extended monocyte population based on FSC vs SSC, and doublet cells (FSC-A vs FSC-H, SSC-A vs SSC-H, and FSC-H vs FSC-W) and dead cells (FSC-A vs 7-aad) were excluded. The left dot plot demonstrates expression of lineage (CD3, CD56, CD19) and HLA-DR, and a population of HLA-DR $^{-}$lineage^{-} is gated (the red circle). MDSCs were defined as HLA-DR^{-}lineage^{-}CD33^{+}CD11b^{+} cells (the upper right dot plot). MDSCs were further classified as CD14^{-}CD15^{-} (e-

MDSC), $CD14^{+}CD15^{-}$ (M-MDSC), and $CD14^{-}CD15^{+}$ (PMN-MDSC) (the lower right dot plot). Representative data from sample no. IT071 v1 is shown. (B) Each subset of MDSCs were sorted by flow cytometry and stained with Giemsa stain. (C) The line graph demonstrates changes with time in MDSC numbers per 1 μl of peripheral blood, which we obtained in sequential sampling, after ITx in individual patients. Numbers of MDSCs increased in 9 of 12 ITx patients (black lines, n = 9), but not in three of them (red lines). The Y-axis is arranged in three segments with different scales to easily visualize the changes in MDSC numbers. (D–G) Graphs demonstrate the total MDSC number (D) and the numbers of PMN-MDSCs (E), e-MDSCs (F), and M-MDSCs (G) per 1 μl of peripheral blood of ITx patients during the pre-transplant period (before Tx, n = 14, circles), within 2 months (period I, n = 10, squares), 2 months to 1 year (period II, n =31, triangles), and more than 1 year (period III, n = 11, reverse triangles) after ITx. Each dot represents individual data, and horizontal lines represent the mean numbers. Statistical significances are indicated in the graphs (Mann-Whitney U test).

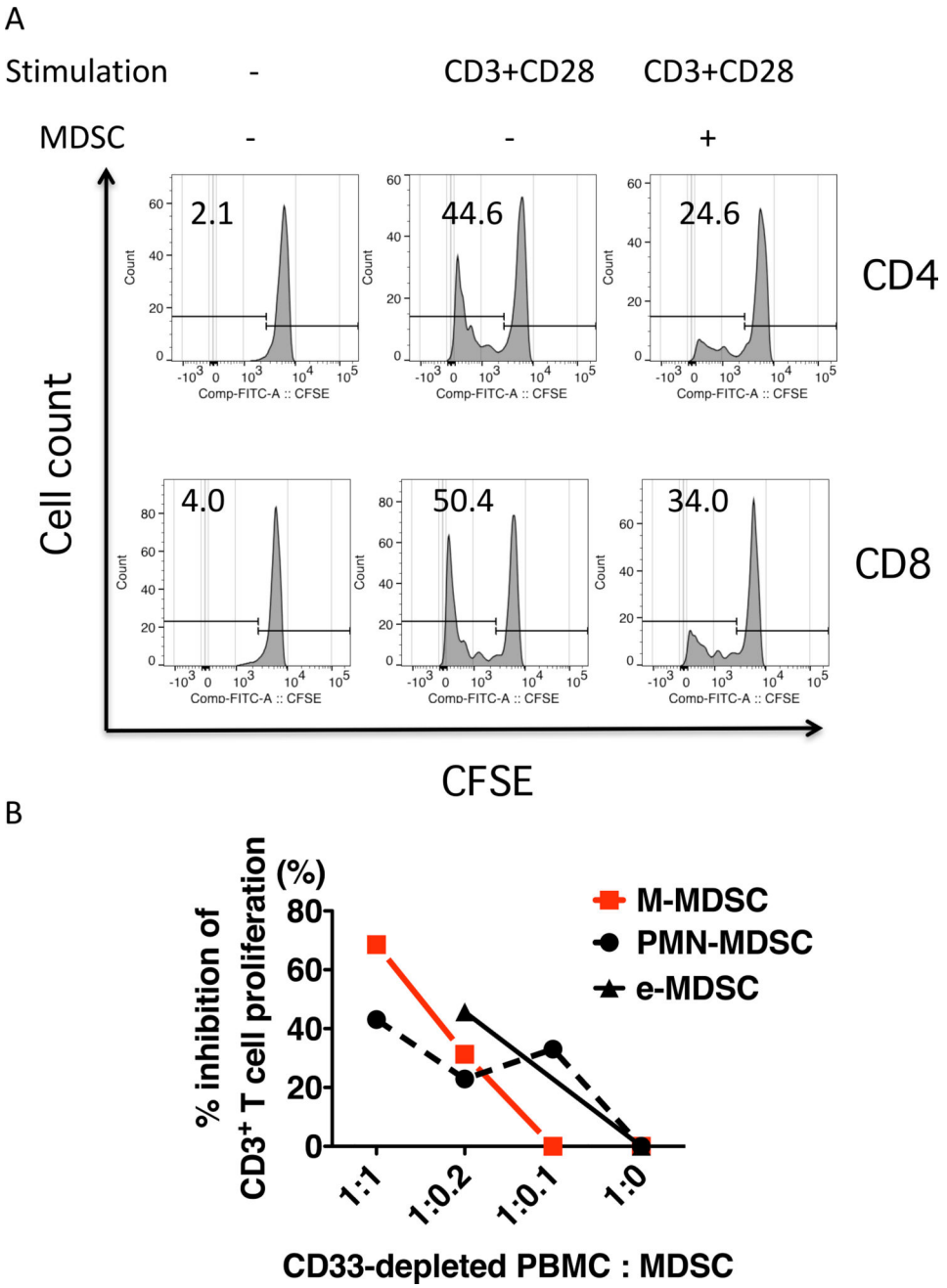

Figure 2. Cells with MDSC phenotype suppress T cell proliferation

CFSE-labeled, magnetically CD33-depleted PBMCs (1×10^5) during the pre-transplant period were stimulated with plate-coated anti-CD3 and anti-CD28 antibodies in 200 μl of T cell-proliferating complete medium in a flat bottom 96-well plastic plate (center and right histograms). For negative controls, 1×10^5 cells were cultured without antibody stimulation (the left column). MDSCs enriched by magnetic beads (the lineage$^-$HLA-DR$^-$ and CD33$^+$ cells) from PBMCs on day 184 after ITx were added into the culture wells (the right histograms: CD33-depleted PBMCs : MDSCs = 5 : 1). Histograms demonstrate fluorescent levels of CFSE in CD4 (the upper histograms) and CD8 (the lower histograms) T cells,

which were gated out as a population of singlet, live $CD3^+CD4^+$ and $CD3^+CD4^+$ cells, respectively. The numbers indicated in the histograms indicate percentages of CFSE-low T cells. Representative data from sample no. IT044 are shown. Similar data were obtained from two other patients. (B) T cells were cultured with or without flow-sorted MDSC subsets, as described in A. The line graph demonstrates percent inhibition of $CD3^+$ T cell proliferation by M-MDSCs (red squares), PMN-MDSCs (black circles), and e-MDSCs (triangles) at the indicated PBMC : MDSC ratios. Representative data from sample no. IT034 on day 458 after ITx are shown. Similar data were obtained from two other patients.

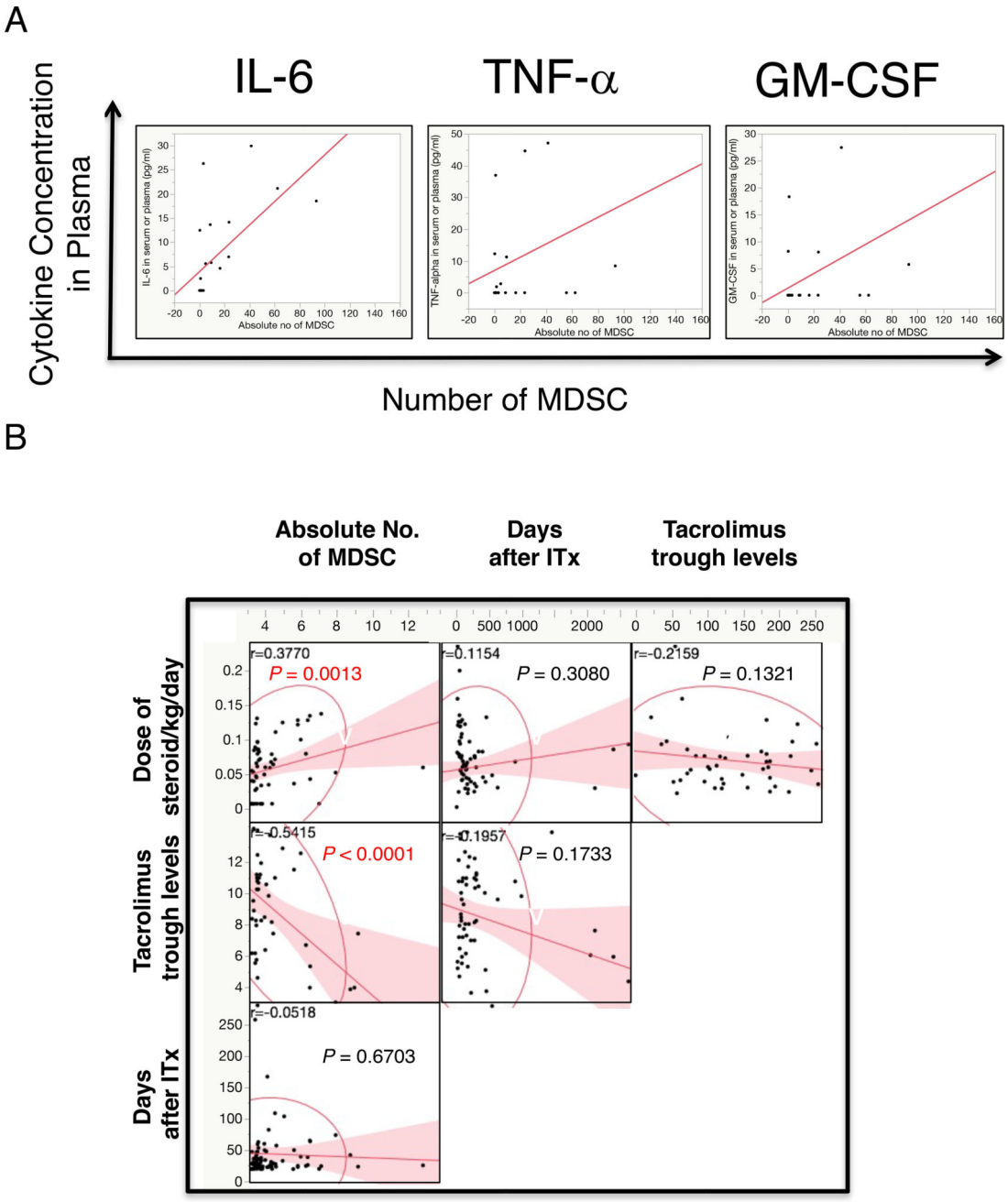

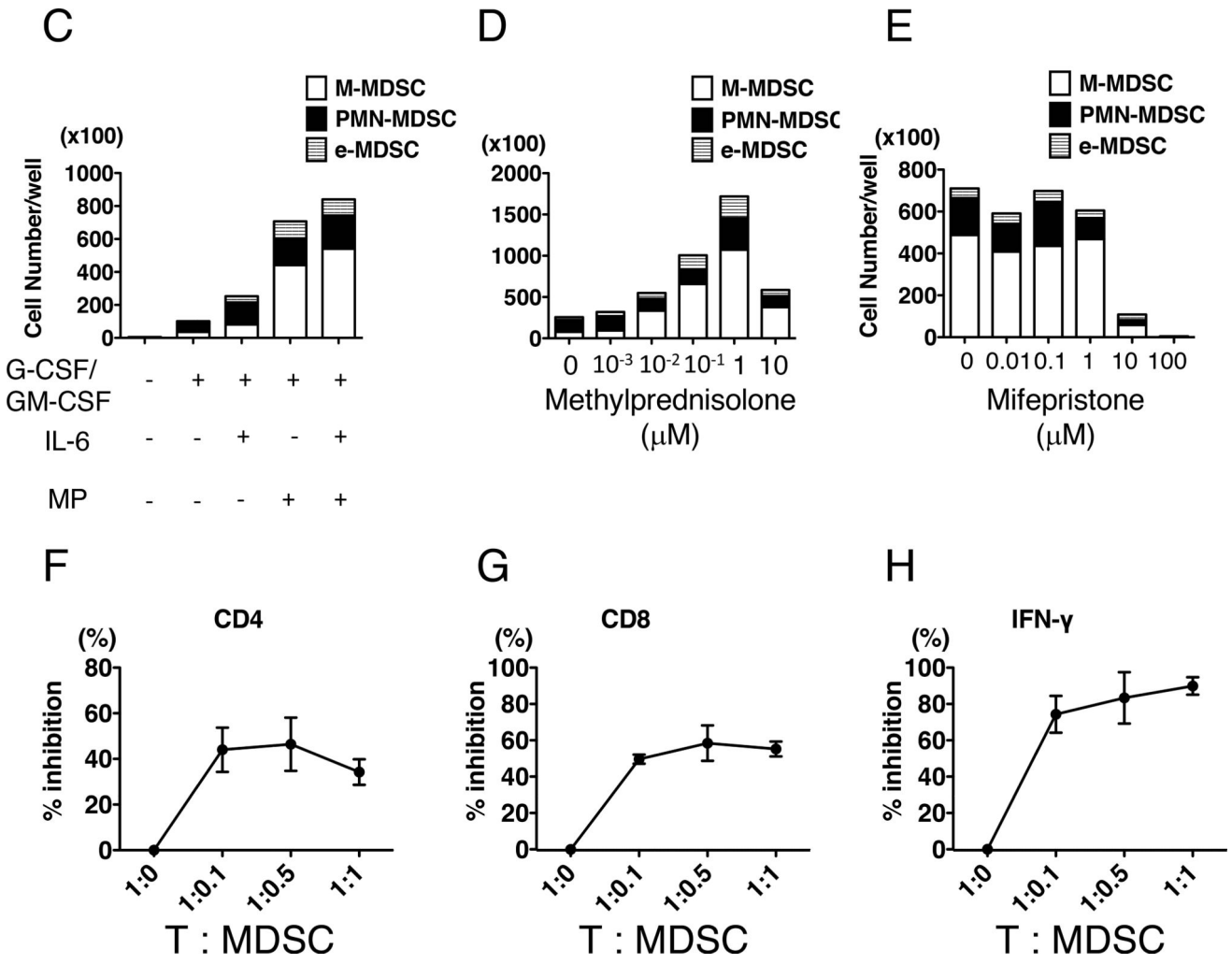

Figure 3. Exogenous steroid hormone and IL-6 are important factors in enhancing MDSC differentiation from BMCs

(A) Cytokines levels in plasma were measured, and linear regression analysis was performed. The scatter plots demonstrate correlation between MDSC numbers and plasma IL-6 levels (left), TNF-α (middle) and GM-CSF (right). Plasma IL-6 levels (Y) (X; r = 0.6888, p = 0.0278, correlation: Y = 3.8703 + 0.2420 X, n = 14), but not TNF-α (p = 0.3638, n = 15) and GM-CSF (p = 0.1942, n = 12), were moderately correlated with MDSC numbers. (B) Correlations between administered doses of steroid [normalized value/body weight (kg), n = 72], tacrolimus trough levels (n = 55), days after transplantation (n = 72), and absolute numbers of MDSCs were investigated using multiple linear regression analysis. The Spearman's rank correlation coefficient (r) and p values are indicated in each scatter plots, and the red lines show fitted linear lines. (C–E) The bar graph demonstrates the numbers of M-MDSCs (white bars), PMN-MDSCs (black bars), and e-MDSCs (striped bars). BMCs were cultured for 6 or 7 days. Representative data from two independent experiments are shown. Culture medium was supplemented with G-CSF and GM-CSF, IL-6, and/or MP (C), with G-CSF, GM-CSF, IL-6 and various concentrations of MP (D), or with G-CSF, GM-CSF, IL-6, MP, and various concentrations of mifepristone (E), as indicated

under the X-axis of the bar graphs. (F–H) CFSE-labeled, CD33-depleted mononuclear cells from BMCs were cultured with a cocktail of irradiated allogeneic B cells and flow-sorted autologous BMC-derived MDSCs at the indicated T : MDSC ratios under the X-axis. Proliferation of $CD3^+CD4^+$ (F) and $CD3^+CD8^+$ (G) cells and IFN-γ production in the cultured medium (H) were measured. The graphs demonstrate % inhibition compared to data from co-culture without MDSCs. Representative data from two independent experiments are shown.

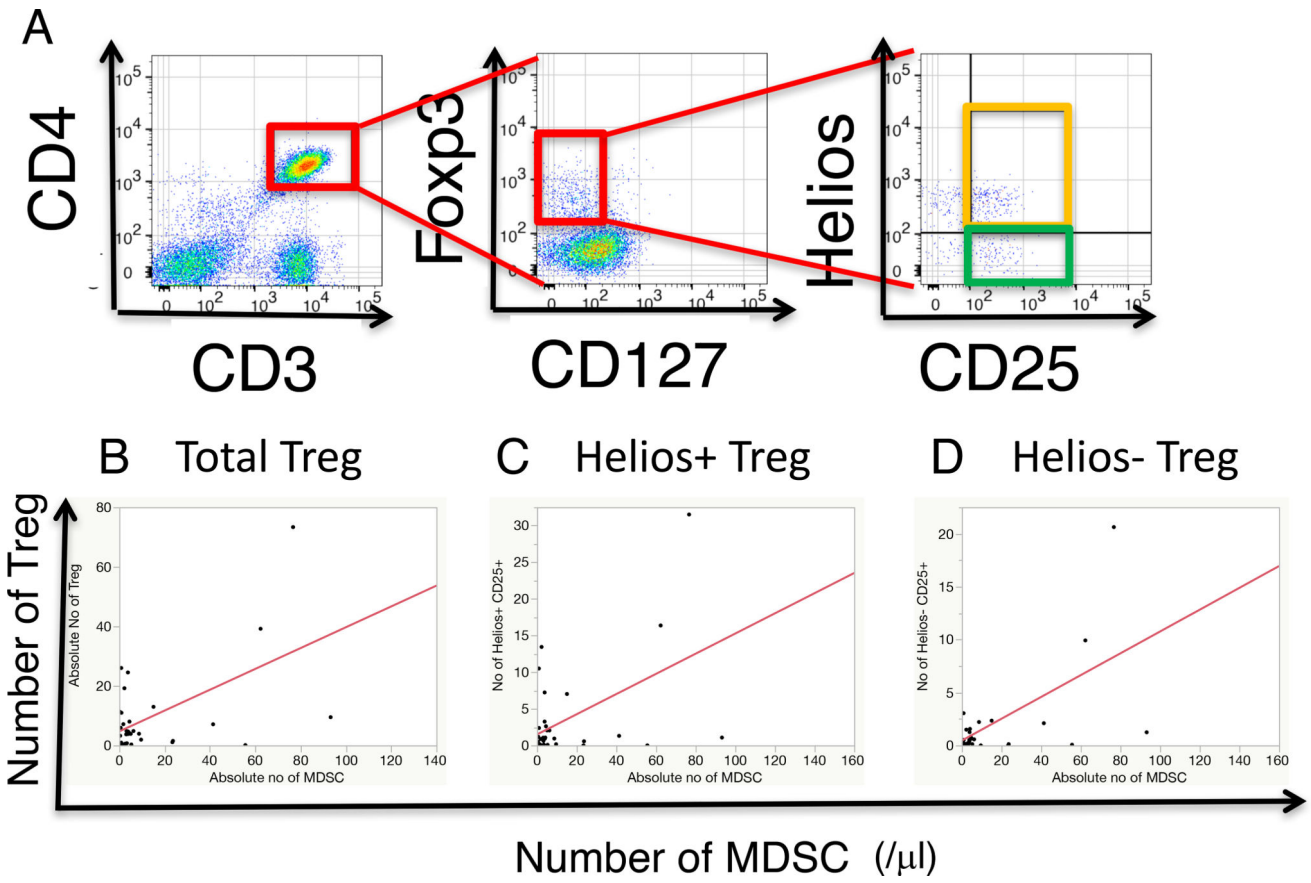

Figure 4. Correlation between the number of MDSCs and the numbers of Treg cells in PBMCs

(A) Dot plots show representative Treg populations in PBMCs. The single and live $CD3^{+}CD4^{+}CD127^{-}Foxp3^{+}C25^{+}$ cells were defined as a Treg population. Two subsets of Treg cells, $Helios^{+}$Treg and $Helios^{-}$Treg, were detected (the right panel). Representative data was from PBMCs of patient no. IT034. (B–D) The scatter plots show correlation between the numbers of MDSC and the numbers of total Treg (B, n = 23, p =0.0056, r = 0.5584, Y = 4.7115 + 0.3497 X), $Helios^{+}$Treg (C, n = 23, p = 0.0263 r = 0.4622, Y = 1.8885 + 0.1320 X), and $Helios^{-}$Treg (D, n = 23, p =0.0023, r = 0.6029, Y = 0.3904 + 0.1039 X) cells in PBMCs.

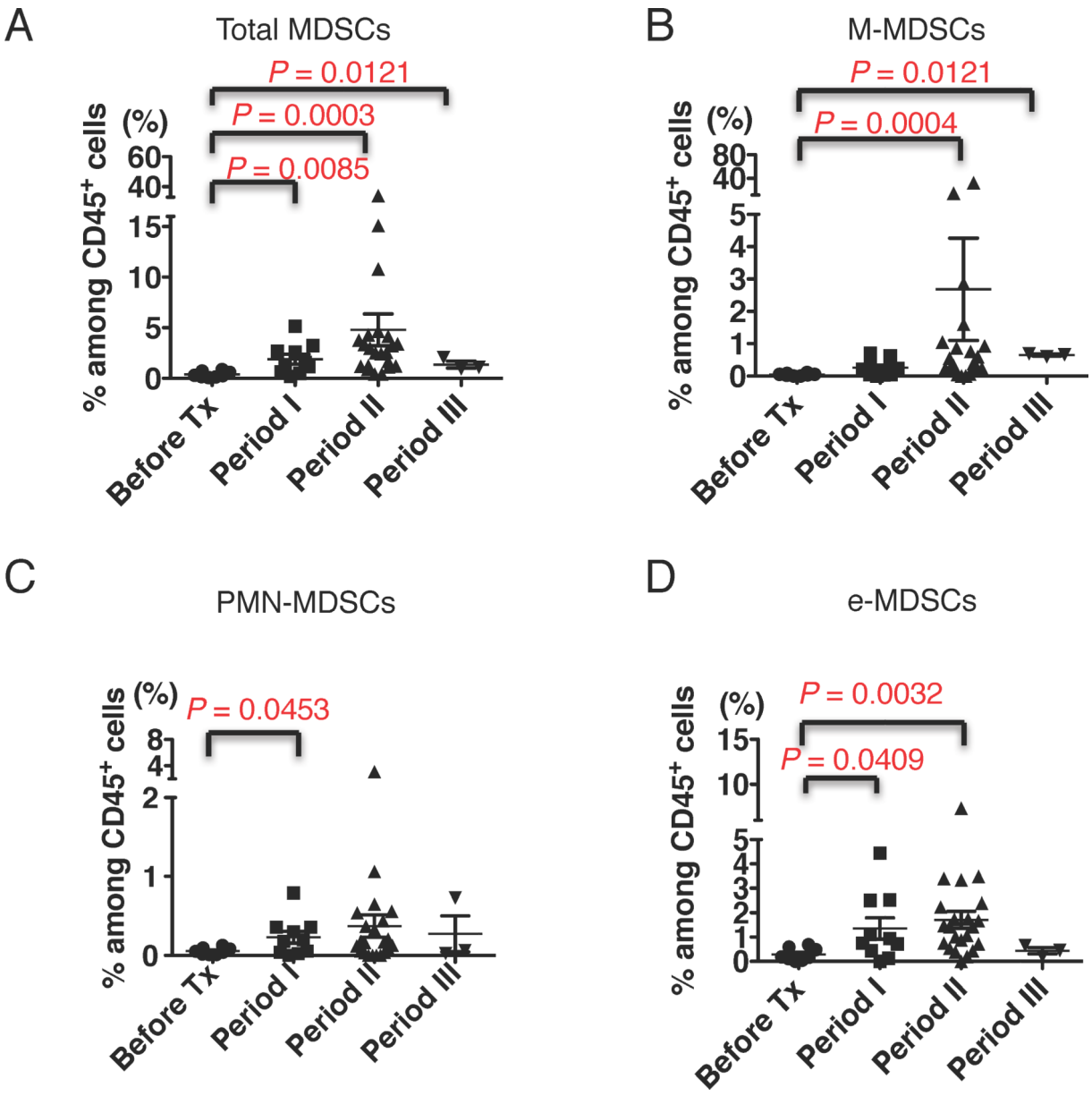

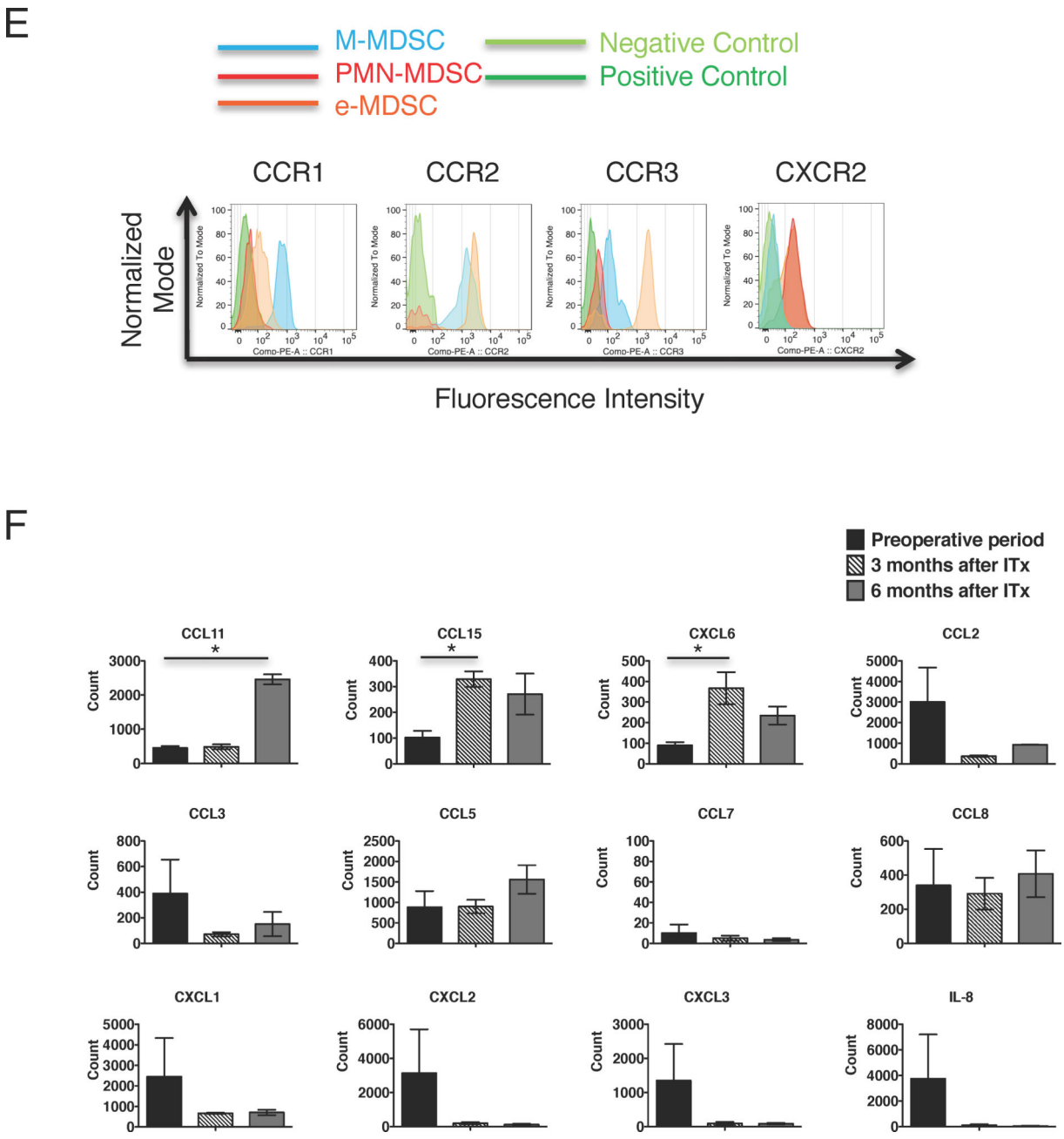

Figure 5. MDSCs increase in allograft intestinal mucosa after ITx

(A–D) MDSCs infiltrating in LPC were detected as shown in Figure S5 and the Materials and Methods. The scatter plots show the percentages of total MDSCs (A), M-MDSCs (B), PMN-MDSCs (C), and e-MDSCs (D) among $CD45^+$ mononuclear cells of LPC during the pre-transplant periods (before Tx, n = 8, circles), within 2 months (period I, n = 10, squares), 2 months to 1 year (period II, n =22, triangles), and more than 1 year (period III, n = 3, reverse triangles) after ITx. Each dot shows individual data of MDSCs, and horizontal lines show the mean percentage ± SEM. Statistical significances are indicated in the graphs (Mann-Whitney U test). (E) The histograms show expressions of CCR1, CCR2, CCR3, and CXCR2 on M-MDSCs (blue), PMN-MDSCs (red), e-MDSCs (orange) and internal negative

(light green) and positive (dark green) controls, which are expected not to express and to express each chemokine receptors, respectively. Similar results were obtained from 5 to 10 different recipients. (F) mRNAs were extracted from pre-transplant grafts (black bar, n = 3), intestinal grafts at 3 months (striped bar, n =3), and those at 6 months (gray bar, n = 2) after ITx and were analyzed using nanoStrings® system. Bar graphs show the mean normalized counts of mRNA ± SEM for indicated chemokine ligands. The statistical *p* values were calculated using a one-way ANOVA with Bonferroni post hoc tests and are indicated in the graphs (* $p < 0.05$).

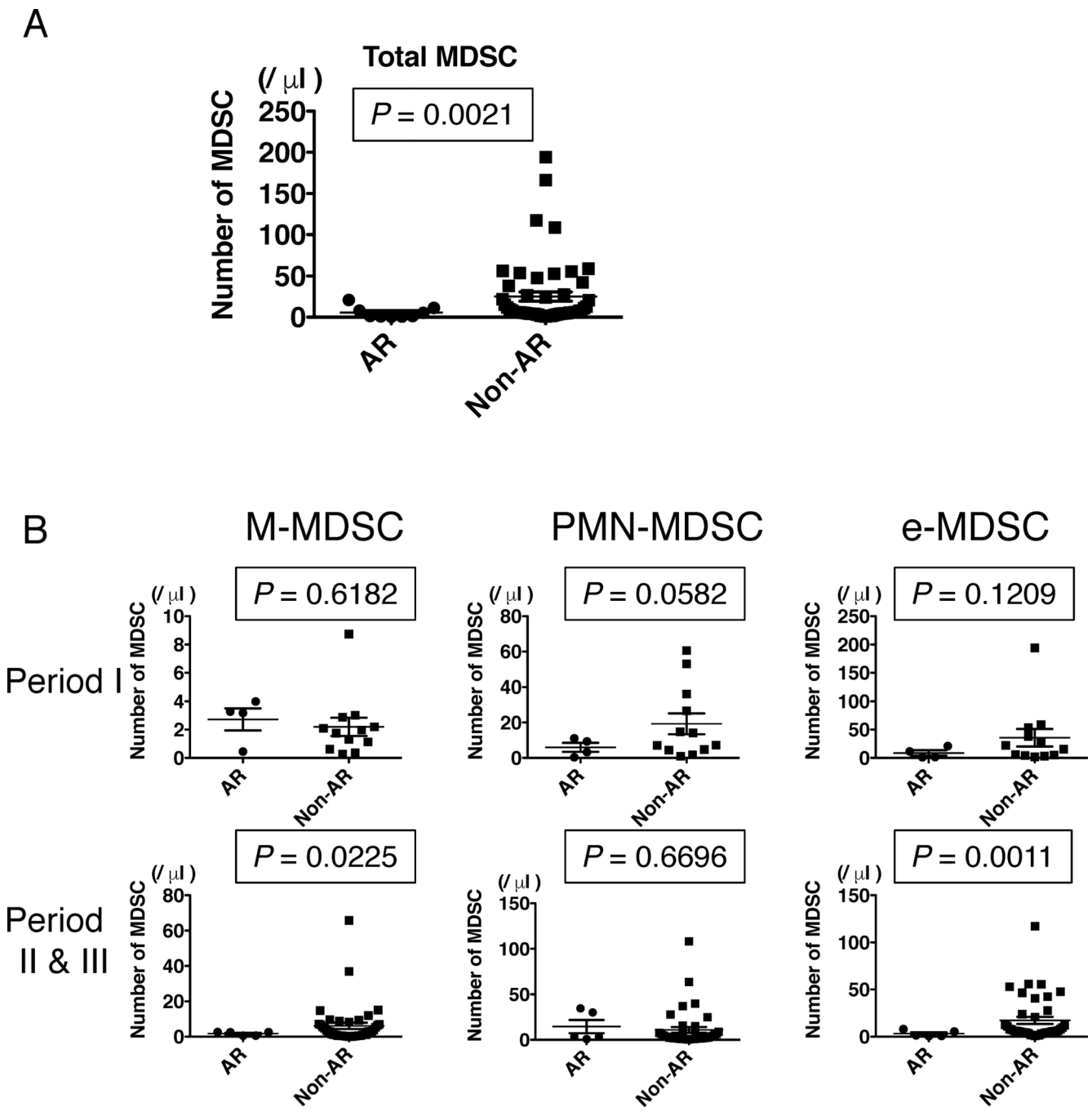

Figure 6. Numbers of MDSCs in PBMCs from recipients with ACR are lower than those from recipients without ACR

(A) Scatter plots show the total numbers of MDSCs in the PBMCs of ITx patients with ACR (circles, n = 9) and those without ACR (squares, n = 50) after ITx. (B) Scatter plots show the numbers of M-MDSCs (the left), PMN-MDSCs (the middle), and e-MDSCs (the right) in the PBMCs of ITx patients with ACR and those without ACR within 2 months (the upper plots, patients with ACR; n = 4; circles, patients without ACR; n = 12; squares) and more than 2 months (the lower plots, patients with ACR; n = 5; circles, patients without ACR; n = 38; squares) after ITx. Each dot shows individual data of MDSCs and horizontal lines show

mean number ± SEM. Statistical significances are indicated in the graphs (Mann-Whitney U test).

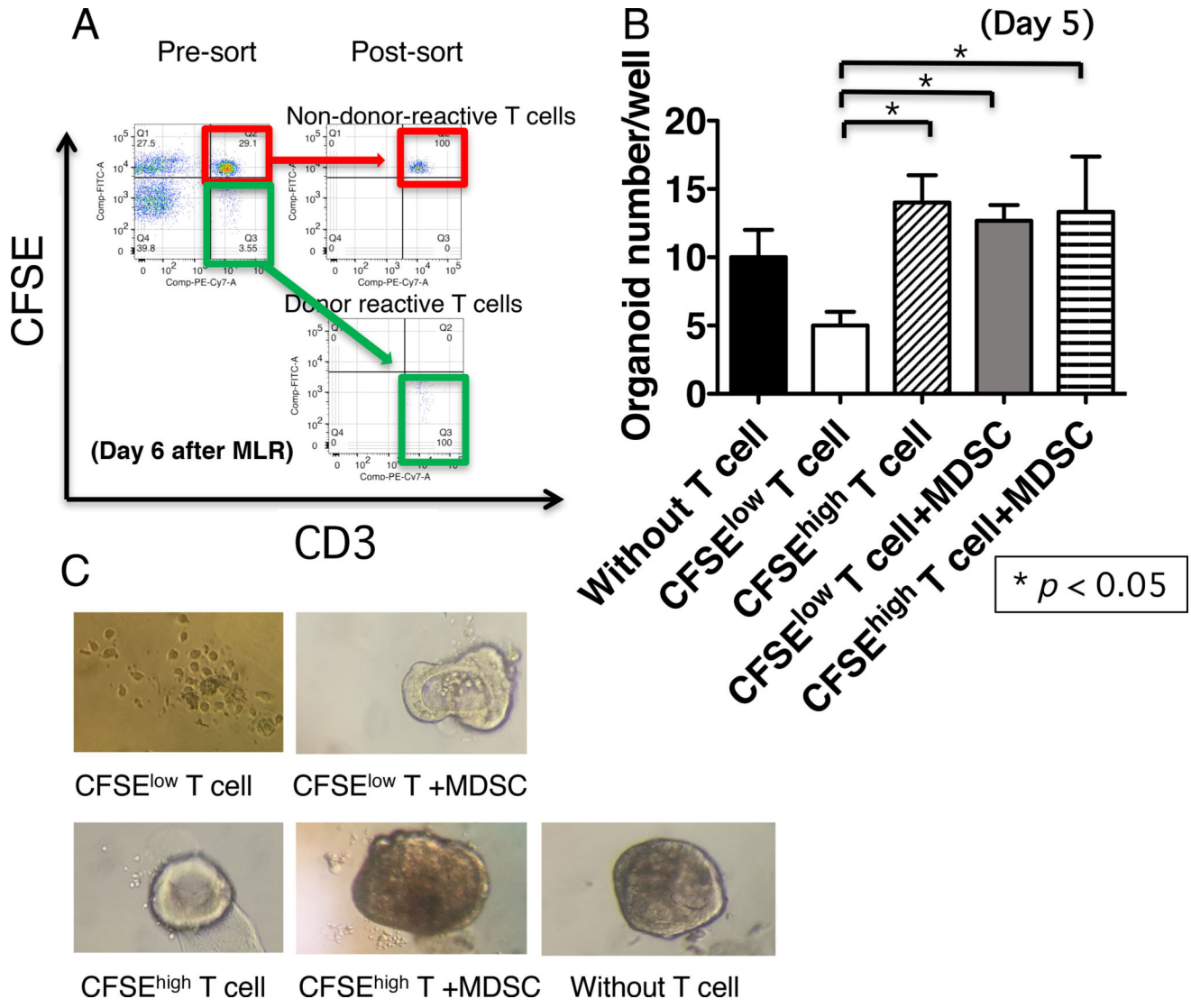

Figure 7. MDSCs suppress donor-reactive T cell-mediated damage of intestinal epithelial organoids

(A–C) CFSE-labeled PBMCs (10×10^4/200 μl/well) from a recipient and the irradiated donor B cells (5×10^4/200 μl/well) were co-cultured for 6 days (total of 52 wells of a 96-well plate), and $CFSE^{low}$ T cells (green square in A) and $CFSE^{high}$ T cells (red square in A) were sorted by a flow cytometer. Donor epithelial organoids were obtained from a biopsy sample, and 100 fragments of passaging organoids were cultured with 1×10^4 flow-sorted $CFSE^{low}$ T cells (gray bar in B and the upper right photograph in C, n = 3) or 1×10^4 $CFSE^{high}$ T cells (horizontal-striped bar in B and the lower middle photograph in C, n = 3) with 1×10^4 sorted MDSCs from PBMCs of the same patient in 30 μl of Matrigel®. As controls, the passaging organoids were cultured in Matrigel® alone (black bar in B and the lower right photograph in C, n = 3) or with the flow-sorted $CFSE^{low}$ T cells (white bar in B and the upper left photograph in C, n = 3) or $CFSE^{high}$ T cells (oblique-striped bar in B and the lower left photograph in C, n = 3). After 5 days of co-culture, the numbers of viable organoids in each well were counted. The bar graph indicates the mean numbers of

organoids ± SEM. Asterisks show significant differences between the indicated groups ($p < 0.05$, one-way ANOVA with Bonferroni post hoc tests). Data are from patients no. IT056. Similar results were obtained in three independent experiments from three different ITx cases.